



Investigation of methane oxidation by palladium-based catalyst via ReaxFF Molecular Dynamics simulation

Qian Mao^a, Adri C.T. van Duin^b, K.H. Luo^{a,c,*}

^a Center for Combustion Energy, Key Laboratory for Thermal Science and Power Engineering of Ministry of Education, Department of Thermal Engineering, Tsinghua University, Beijing 100084, China

^b Department of Mechanical and Nuclear Engineering, The Pennsylvania State University, University Park, PA 16802, USA

^c Department of Mechanical Engineering, University College London, Torrington Place, London WC1E 7JE, UK

Received 3 December 2015; accepted 15 August 2016

Available online 13 October 2016

Abstract

Catalytic oxidations of methane over palladium-based nanoparticles, with and without oxygen coating, are investigated using ReaxFF Molecular Dynamics simulations. The simulation results show the complete dynamic process of the above catalytic reactions at the atomic level and help to reveal the underlying mechanisms both qualitatively and quantitatively. It is found that oxygen molecules are significantly easier to be adsorbed on both bare and oxygen-coated Pd surfaces compared with CH₄. The presence of adsorbed O₂ molecules on the surface blocks the active sites for CH₄ adsorption on the oxygen-coated Pd surfaces. By comparing the adsorptive dissociation of CH₄ over Pd nanoparticles with different levels of oxygen coverage, we find that it is much easier for the adsorptive dissociation of CH₄ on oxygen-coated Pd nanoparticles than that on bare Pd nanoparticles at low temperatures. In contrast to the rapid dissociation of CH₄ after adsorption, the dissociation of O₂ requires much higher temperature than adsorption. Moreover, the CH₄ dissociation rate increases with the rising temperature and is sensitive to the level of oxygen coverage on the surface. In addition, the activation energies for the adsorptive dissociation of CH₄ are determined by fixed-temperature simulations from 400 to 1000 K through the changes of CH₄ concentration and are found to be 3.27 and 2.28 kcal mol⁻¹ on 0.3 and 0.7 ML oxygen-coated Pd nanoparticles, respectively, which are consistent with density functional theory calculations and experiments.

© 2016 by The Combustion Institute. Published by Elsevier Inc.

Keywords: Methane; Palladium-based catalyst; ReaxFF Molecular Dynamics; Catalytic reaction

1. Introduction

Oxidation of methane to carbon dioxide and water over palladium-based catalysts has been studied extensively for the recent decades [1–3]. The lower carbon-to-hydrogen ratio in methane reduces the emission of CO₂ compared with other hydrocarbon-based fuels per unit of produced

* Corresponding author at: Department of Mechanical Engineering, University College London, Torrington Place, London WC1E 7JE, UK. Fax: +44 (0)20 7388 0180.

E-mail addresses: K.Luo@ucl.ac.uk, prof.k.h.luo@gmail.com (K.H. Luo).

energy. In addition, it has higher heat sink capacity and specific energy content than jet fuels [4]. However, methane possesses the greatest C–H bond strength among all the saturated hydrocarbons with a H–CH₃ bond dissociation energy of 104 kcal mol⁻¹, which leads to the poor ignition performance for gas phase reactions [2]. Conversely, the activation energy for CH₄ dissociation on some novel metals (Pd, Pt, Rh, Ni) can be as low as 7–10 kcal mol⁻¹. Among them palladium is regarded to be the most promising for complete CH₄ oxidation at low temperatures [5–8]. This provides an attractive alternative to the gas phase reaction and satisfies the ultralow NO_x emission in advanced gas turbines, reduces the emission of CO and soot in industrial applications, e.g., automotive vehicles, improves the low-temperature ignition performance of supersonic engines with limited residence time, and extends the flame stabilization limits in counter-current-channel combustors [9–13].

Changes in the morphology, synthesis method, size as well as oxidation state of the catalyst all contribute to the variations in activity for methane oxidation. In situ generated Pd nanoparticles were tested experimentally and numerically revealing that key surface reaction steps were the reversible oxygen adsorption/desorption [4]. Law et al. utilized a Pd wire covered with a PdO surface layer to study the methane oxidation and narrowed the global energy barrier down to 21.5 ± 0.9 kcal mol⁻¹ [14,15]. Since an ideal catalyst should have low temperature activity yet high-temperature stability, supported palladium based catalysts are regarded to be resistant to sintering at high temperatures. The methane reaction over strontium-palladium-substituted hexaluminate catalyst was found to have higher activity and anti-sintering capability than hexaluminate catalyst [16,17]. Li et al. developed a stagnation swirl flame to synthesize Pd/TiO₂ nano catalysts, which exhibited excellent activity for methane oxidation [18,19]. Al₂O₃ was also commonly used as support for Pd nanoparticles [20,21].

During methane combustion, operating and exposing to oxygen, palladium-based catalysts are likely to be oxidized and form surface and even some bulk oxide phase, which significantly alter the activity, selectivity, stability as well as turnover rate [22–24]. The nature of the active sites on palladium for the methane dissociation, however, has remained as a subject of debates despite numerous studies. The conversion between PdO and Pd had a profound effect on the reaction rate during heating-cooling cycles [19,25–27]. According to TEM studies [21] and Mars and van Krevelen mechanism [28], the oxidation of methane was supposed to mainly occur on the site pairs consisting of both oxygen atoms (Pd oxide) and oxygen vacancies (metallic Pd). Furthermore, molecular beam

studies indicated that oxygen blocks sites for dissociative adsorption [29,30]. Catalytic enhancement of methane ignition on palladium caused heat release and temperature rise after dissociative adsorption of methane and then accelerated chain-branching. According to the DFT and in situ SXRD studies [2,31–33], dissociative adsorption of methane was regarded as the rate-limiting step.

All above demonstrate the complex nature of methane combustion on palladium-based catalysts, and that the underlying mechanisms remain unclear. Finding a more effective state of Pd-based catalysts and clarifying the mechanisms require understanding of these issues at the atomic level. Quantum mechanics (QM) simulations, e.g., ab initio MD is still limited to fs–ps timescales and small systems (~100 atoms). An attractive alternative approach is the molecular dynamic simulations based on the ReaxFF force field, which is capable of describing the dynamic process of chemical reactions for a much larger system [34]. In previous studies, e.g., [35], the reaction mechanisms, activation energies, and rate constants of combustion and pyrolysis obtained from ReaxFF MD simulations were found to be in good agreement with available experimental data. The objective of the present study is to understand the influence of oxygen coverage on Pd nanoparticles on the methane oxidation as well as to explore the underlying gas-surface reaction mechanisms. Therefore, the interplay between the catalyst and the gas phase molecules of O₂ and CH₄, jointly and separately, is scrutinized. That is, we consider systems of CH₄/O₂ mixture reacting over Pd nanoparticles of bare and oxygen-coated surfaces and systems of CH₄ molecules reacting over the above Pd-based catalysts. Reaction rate and the activation energy of CH₄ dissociation on the oxygen-coated Pd nanoparticles are quantitatively determined from the ReaxFF MD simulations.

2. Method

2.1. Simulation method

Molecular dynamics simulation based on ReaxFF force fields is adopted for the heterogeneous catalytic reaction. In contrast to the empirical non-reactive force field that features the pre-defined rigid connectivity between atoms, the ReaxFF force field is based on bond-length/bond-order combined with polarizable charge to describe covalent, Coulomb, and van der Waals interactions [34]. The force field is parameterized against QM-based training sets, making it capable to model the bond breaking and formation during chemical reactions. Therefore, ReaxFF MD is more efficient and accurate than any current semi-empirical method while it is computationally much cheaper than DFT to allow simulations of reactive

processes in larger systems and for longer physical time [36]. Further information on the ReaxFF description can be found in the literatures that address the ReaxFF formalism [34,37]. The Pd/C/H/O ReaxFF force field description has previously been applied to several complex Pd-containing systems, such as palladium oxide [24], palladium hydride [38].

2.2. Simulation details

Molecular dynamics simulations based on Pd/C/H/O ReaxFF force field are performed using canonical ensemble (NVT) to prepare oxygen-coated Pd nanoparticles, study the reactions of CH_4/O_2 mixture and dissociative adsorption of CH_4 on Pd-based catalysts. The size of the box in every simulation is $80 \times 80 \times 80 \text{ \AA}$ and periodic boundary condition is implemented in all three directions. Before MD simulations, every system is firstly energy minimized via a conjugate gradient algorithm to eliminate simulation artifacts that can arise from initial high energy contacts. A time step of 0.25 fs is selected to ensure energy conservation at the temperatures used in this study. Then the catalyst is equilibrated to the reaction temperature for 1×10^5 iterations by the Nosé–Hoover thermostat with a damping constant of 100 fs prior to any reactive simulation. The ReaxFF MD simulation is performed using a ReaxFF code as implemented in the Large-scale Atomic/Molecular Massively Parallel Simulator (LAMMPS) package [39]. All of the system configurations and snapshots in this study are prepared using the Visual Molecular Dynamics (VMD) software [40].

3. Results and discussions

3.1. Oxygen-coated Pd preparation

Since most catalytic applications feature metal nanoparticles rather than single crystal surfaces, a 3 nm Pd nanoparticle is firstly prepared with 935 atoms. Prior to investigating catalytic reactions, two fixed-temperature NVT-MD simulations are performed to prepare oxygen-coated Pd nanoparticles with different surface coverages. Considering the surface atom number of 332 for a 3 nm Pd nanoparticle, two different oxygen molecule numbers, that is, 200 and 80 are distributed randomly in the simulation box. Details about the system configuration of the high density case is displayed in Fig. 1a with a 3 nm Pd nanoparticle placed in the center of a simulation box and 200 oxygen molecules around it.

During the oxidation process, the temperature is controlled at 1500 K for both cases, which is high enough to yield oxygen dissociation on Pd surfaces in the simulation timeframe, but is low enough to maintain a crystalline lattice in the bulk [24].

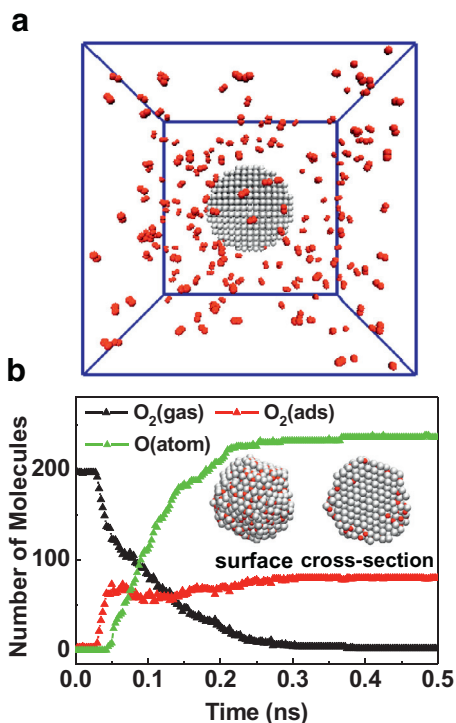


Fig. 1. NVT simulations of the preparation of oxygen-coated Pd nanoparticles: (a) Initial configuration (b) Number of molecules.

The simulations are performed using a velocity-Verlet [39] approach to update velocities and positions up to 2×10^6 iterations (0.5 ns). The number of O_2 molecules and O atoms in the gas phase or adsorbed on the Pd surface, respectively, are recorded and the resulting species population plots are shown in Fig. 1b. It is observed that the dissociation of O_2 happens after the Pd surface gets saturated with the adsorbed O_2 . After 0.3 ns, the numbers of these three species are stable, meaning the oxidation process is equilibrated. The inset snapshots present the final configurations of the oxidized nanoparticle viewed on the surface and cross-section, which are extracted from the simulation box with the adsorbed O_2 molecules being removed from the surface. Obviously, the majority of the dissociated O atoms are located on the surface. As a result, two oxygen-coated Pd nanoparticles with oxygen coverage of 0.7 and 0.3 ML (ML = adsorbed atoms/surface metal atom) are obtained for the later CH_4 oxidation simulations.

3.2. Reaction of CH_4 and O_2 over Pd-based Catalyst

Previous experiments have revealed the energy barrier for methane oxidation over PdO is lower than that over bare Pd and the ignition

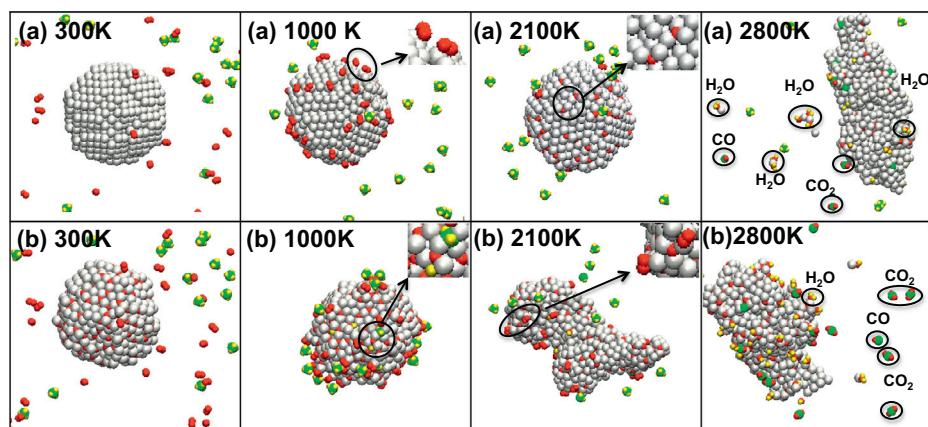


Fig. 2. Snapshots from temperature ramp simulations of CH_4/O_2 mixture over (a) bare and (b) oxygen-coated Pd nanoparticles (color code: green = carbon, yellow = hydrogen, red = oxygen, white = palladium). (For interpretation of the references to color in this figure legend, the reader is referred to the web version of this article.)

temperature is about 600 K [14,15,18]. However, it is impractical to perform the MD simulations up to the time scales used in the experiments (~ 30 min) due to the limitations of available computational resources [41]. To ensure that the reaction takes place at nanoscales in the ReaxFF MD simulations, a high initial gas phase pressure is required. Therefore, 40 molecules of O_2 and 20 molecules of CH_4 in the gas phase with an initial equivalence ratio of 1 and pressure of 4.85 atm are adopted. Temperature ramping NVT MD simulations are employed to assess reactivity of CH_4/O_2 mixture over bare and oxygen-coated Pd nanoparticles and reveal the interplay between O_2 and CH_4 with the catalysts.

The reaction temperature is initially set at 300 K and is increased at a rate of 1.08 K/ps, yielding a final temperature of 3000 K after 1×10^7 iterations. Molecules in the gas phase are initially given the velocities in Gaussian distribution at 300 K and the equilibrated nanoparticle is located in the center of the simulation box. Figure 2 depicts the dynamic reactions on (a) bare and (b) oxygen-coated (0.7 ML) Pd nanoparticles. The intermediate species in CH_4 oxidation are quite complicated, so only the key species are considered. The resulting species population plots for the above two simulations are demonstrated in Fig. 3a and b. Combining Fig. 2 with Fig. 3, the catalytic reaction steps for CH_4/O_2 mixture over Pd-based catalysts can be summarized as follows: (i) adsorption of O_2 until the catalyst surface getting saturated; (ii) dissociation of the adsorbed O_2 with rising temperature; (iii) dissociative adsorption of CH_4 at high temperatures; (iv) formation of CO_2 , H_2O , etc. and desorption back to the gas phase.

It is noteworthy that at 1000 K in Fig. 2, in contrast to CH_4 , all the O_2 molecules in gas phase are adsorbed by both bare and 0.7 ML oxygen-coated Pd nanoparticles. This confirms that CH_4

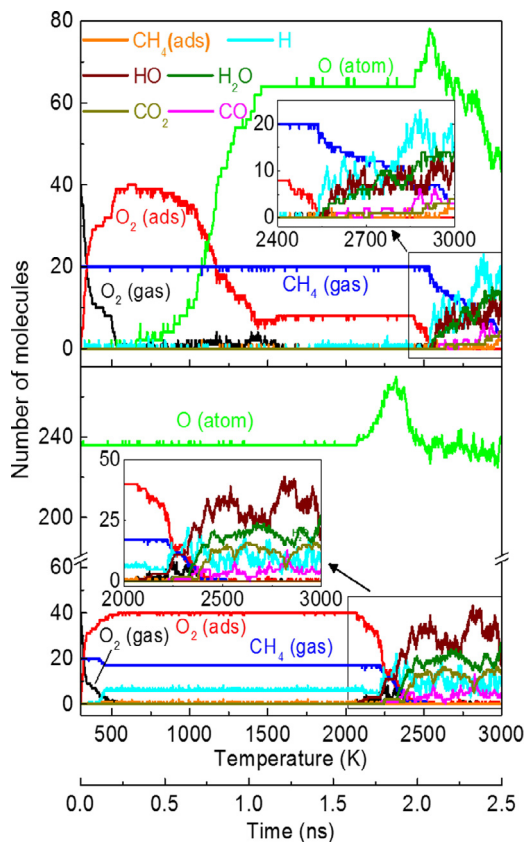


Fig. 3. The number of molecules during temperature ramp simulations of CH_4/O_2 mixture over (a) bare and (b) oxygen-coated Pd nanoparticles corresponding to Fig. 2.

molecules are less active when competing for active sites with O_2 molecules on Pd-based catalyst surface. Specifically, for reaction (b), during the adsorption of O_2 molecules below 1000 K, some CH_4 molecules dissociate into fragments on the surface, resulting in CH_3 , CH_2 and H radicals, etc. Then after all the gas phase O_2 have been adsorbed on the surfaces, no CH_4 adsorption or dissociation is observed until $T \sim 2500$ K for reaction (a) and ~ 2200 K for reaction (b), respectively. The dissociation of the adsorbed O_2 for reaction (a) begins at ~ 700 K and some adsorbed O_2 also desorb back into the gas phase as temperature increases. Subsequently, the dissociated O atoms and adsorbed O_2 molecules reach equilibrium on the surface as shown in Fig. 2a at 2100 K. However, there are still a lot of adsorbed O_2 on oxygen-coated Pd nanoparticle at 2100 K in Fig. 2b. A massive dissociation happens until the temperature rises to ~ 2200 K, with the significant change of the nanoparticle morphology. This difference can be attributed to surface oxygen coverage effects, as the energy barrier of O_2 dissociation over Pd (111) increases from $17.1 \text{ kcal mol}^{-1}$ at 0.22 ML to $25.14 \text{ kcal mol}^{-1}$ at 0.5 ML [24,42,43]. With the increase of temperature, the O_2 and CH_4 all dissociate and substantial amounts of OH, H_2O , CO_2 , CO form rapidly over 2200 K on the oxygen-coated Pd nanoparticle. But for the bare Pd nanoparticle, it happens at about 2500 K. This delay results from the different melting points of Pd and PdO. In other words, a higher surface coverage of oxygen atoms leads to a lower melting point. Moreover, as illustrated in Fig. 2b at 2100 K, changes in morphology are dramatic for the oxygen-coated Pd nanoparticle, which provides more active sites for the dissociative adsorption of CH_4 , consequently accelerating the chain-branching. Therefore, it underlines the fact that the dissociative adsorption of CH_4 is the rate-limiting step for methane oxidation [2,14,31–33]. As a comparison, an additional homogeneous gas phase CH_4/O_2 simulation is performed in the absence of Pd-based NPs with the same initial settings as reactions (a) and (b), in terms of the molecule number, equivalence ratio, pressure, temperature, etc. With the same heating rate, this mixture requires an initiation temperature of around 4000 K. For this reason, all the events observed in reactions (a) and (b) can be associated to the Pd-based catalysis.

3.3. Adsorptive dissociation of methane over Pd-based catalyst

Based on the above results, in this section, we focus on investigating the influence of the surface oxidation state on the adsorptive dissociation of CH_4 . Fix-temperature NVT-MD simulations are performed from 400 K to 1000 K with 20 CH_4 molecules in the gas phase. The resulting key species populations of the three reactions at

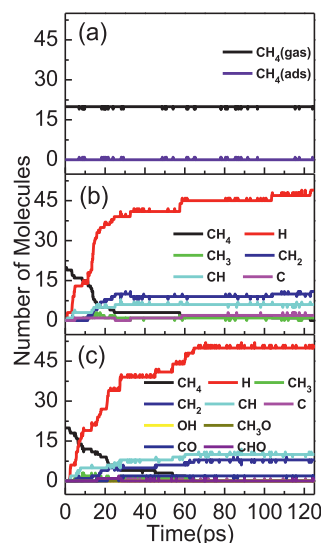


Fig. 4. The number of molecules during fix-temperature NVT-MD simulations of CH_4 over (a) bare (b) 0.3 mL and (c) 0.7 mL oxygen-coated Pd nanoparticles.

$T = 1000$ K are plotted in Fig. 4. Clearly, no CH_4 molecules are found to be adsorbed or dissociate on the bare Pd nanoparticle in the 125 ps simulation window as indicated in Fig. 4a. Additional simulations show the CH_4 adsorptive dissociation on bare Pd nanoparticles happens up to 2500 K. This is consistent with previous experimental results that the metallic palladium itself does not exhibit high activity in methane combustion [2,27]. However, on oxygen-coated surfaces the adsorption and subsequent dissociation of CH_4 are much easier. This confirms that the adsorbed O_2 molecules block the active sites for CH_4 adsorption on oxygen-coated Pd surfaces as observed in molecular beam studies [29,30]. Dissociation rate as well as intermediate species are sensitive to the oxygen coverage on the Pd surface. After dissociation, intermediate species such as CH_3 , CH_2 , CH are formed simultaneously on both cases. Besides, some other species, e.g., OH, CHO and CO are also formed on the 0.7 ML oxygen-coated Pd nanoparticles. This implies that the existence of oxygen on the Pd surface helps the adsorptive dissociation of CH_4 at low temperatures. Furthermore, it gives answer to the dissociation of some CH_4 molecules on the oxygen-coated surface at low temperature in CH_4/O_2 mixture system discussed in Section 3.2. Moreover, the adsorption and dissociation for CH_4 and O_2 are found quite different, that is, CH_4 molecules may dissociate rapidly after adsorption while the dissociation of O_2 requires much higher temperature than O_2 adsorption.

Detailed dynamic process of adsorptive dissociation of CH_4 on the 0.7 ML oxygen-coated

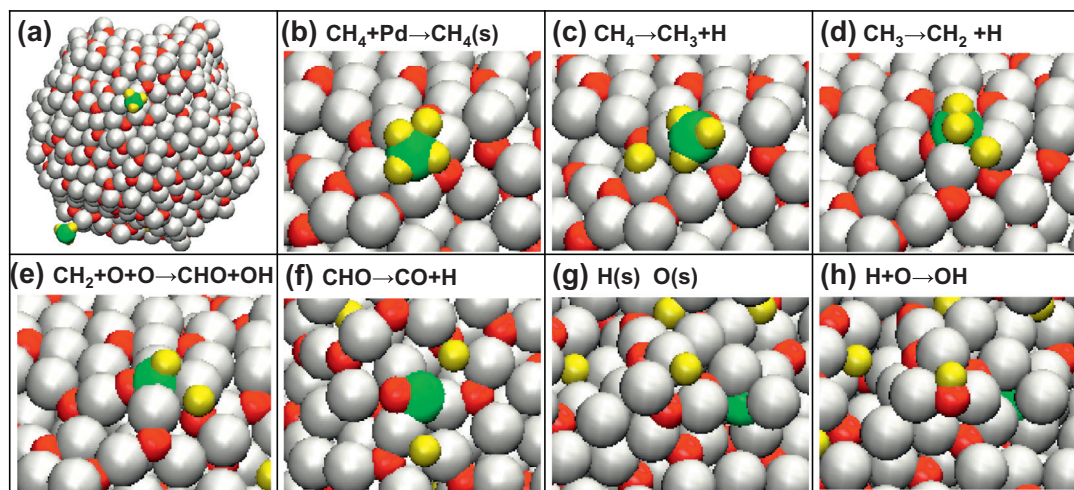


Fig. 5. Snapshots of CH_4 dissociation over the 0.7 ML oxygen-coated Pd nanoparticle.

Pd nanoparticle is displayed through the atomic-level snapshots in Fig. 5. An overview of the initial configuration including the catalyst and CH_4 molecules is shown in Fig. 5a. The dissociation begins after the adsorption of the CH_4 molecule on the surface, with the rearrangement of the four hydrogen atoms to the carbon atom as seen in Fig. 5b. Then the adsorbed CH_4 dissociates to CH_3 and H immediately, with H diffusing to O and CH_3 sticking to Pd. After that, CH_3 diffuses on the Pd surface and dissociates to CH_2 and H . CH_2 may diffuse to react with O , forming CHO and HO . Subsequent dissociation is from CHO to CO and H as shown in Fig. 5f. Adjacent O and H radicals diffuse to form OH radicals afterwards. Since the curve and amorphous surface of the reacted catalyst, it leads to higher energy barriers for H and O to diffuse [24,38], hindering the possibility of the formation of H_2O and CO_2 in our short simulation duration.

3.4. Global kinetic parameters for adsorptive dissociation of CH_4

We utilize the CH_4 consumption rate as a guide to study the first-order kinetics of the adsorptive dissociation of CH_4 over Pd-based catalysts. Figure 6 represents the changes of average CH_4 concentration as a function of simulation time obtained from NVT-MD simulations at temperatures ranging from 400 K to 1000 K over the oxygen-coated Pd nanoparticle at 0.3 and 0.7 ML coverage, respectively. For each temperature, the concentration of CH_4 is averaged at each time point from 5 independent simulations. Clearly, at the initial stages of the simulations, the methane concentration decreases more quickly with the increasing of

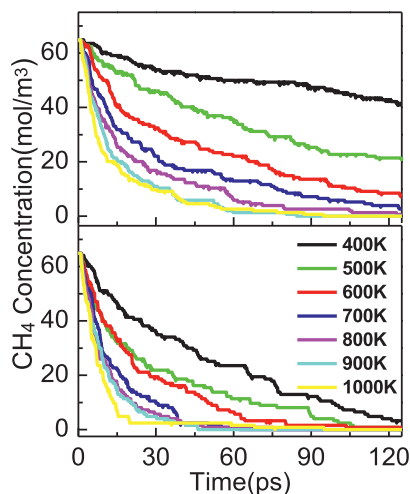


Fig. 6. Changes of the average CH_4 concentration during ReaxFF NVT-MD simulations at various temperatures over 0.3 ML (top panel) and 0.7 ML (bottom panel) oxygen-coated Pd nanoparticles.

temperature and on Pd nanoparticles with higher oxygen coverage.

According to the first-order reaction model, the rate constant, k , at each temperature is determined from a linear fitting to $\ln \frac{[\text{CH}_4]_t}{[\text{CH}_4]_0}$, where $[\text{CH}_4]_0$ and $[\text{CH}_4]_t$ correspond to the concentration of CH_4 initially and at an arbitrary moment t , respectively. From the Arrhenius plot in Fig. 7, distinctive Arrhenius parameters for methane adsorptive dissociation on 0.3 and 0.7 ML oxygen-coated Pd nanoparticle are determined through the two linear fitted lines. The activation energies (E_a) for

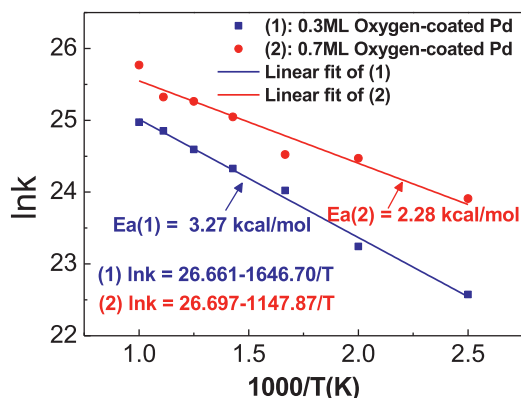


Fig. 7. Determination of activation energies for the dissociation of CH_4 over oxygen-coated Pd nanoparticles from ReaxFF NVT-MD results in Fig. 6.

methane adsorptive dissociation on 0.3 and 0.7 ML oxygen-coated Pd nanoparticle are $3.27 \text{ kcal mol}^{-1}$ and $2.28 \text{ kcal mol}^{-1}$, respectively. The results from the ReaxFF simulations are in good agreement with DFT results by Broclawik et al., for the energy of CH_4 dissociation on linear Pd_2O is $1.0 \text{ kcal mol}^{-1}$ [44] and on PdO diatomic is $3.3 \text{ kcal mol}^{-1}$ [45]. Based on HSE06 and PBE, DFT calculations for methane oxidation over PdO (101) are $6.7 \text{ kcal mol}^{-1}$ and $11.3 \text{ kcal mol}^{-1}$, respectively [46]. In addition, experimental research reveals the activation energy for dissociative adsorption of CH_4 on PdO surface is $21.5 \pm 0.9 \text{ kcal mol}^{-1}$ [14,15], which is also in accordance with our simulation results.

4. Conclusions

Catalytic reactions of both CH_4/O_2 mixture and CH_4 over Pd-based catalysts, with bare and oxygen-coated surfaces, are investigated comprehensively via ReaxFF Molecular Dynamics simulation. The simulation results clearly show the whole dynamic processes of the catalytic reactions at the atomic level to aid the detailed reaction pathway analysis and help to reveal the underlying mechanisms both qualitatively and quantitatively, which would be inaccessible by experiments. In the CH_4/O_2 mixture system, CH_4 molecules are less active to compete for active sites than O_2 molecules on both bare and oxygen-coated Pd surfaces. The adsorbed O_2 molecules block the active sites for CH_4 adsorption on the oxygen-coated Pd surfaces. Furthermore, the dissociation of the adsorbed oxygen molecules on the oxygen-coated surface is much harder than on the bare Pd surface. However, in the simulation of CH_4 reactions on Pd-based catalysts, adsorptive dissociation of CH_4 on bare Pd nanoparticle happens at a much higher temperature than that on oxygen-coated Pd nanoparticles. Moreover,

the CH_4 dissociation rate increases with the rising temperature and is sensitive to the level of oxygen coverage on the surface. In contrast to the rapid dissociation of CH_4 after adsorption, the dissociation of O_2 requires much higher temperature than adsorption. In addition, from the simulations, we conclude that during the catalytic reaction of CH_4 , part of Pd may firstly be oxidized to PdO with rising temperature. Then the coexistence of PdO and Pd on the surface leads to the reduction of activation energy barrier for the adsorptive dissociation of methane, which consequently accelerates the methane ignition. Using a first-order reaction model, the activation energies for CH_4 adsorptive dissociation on 0.3 and 0.7 ML oxygen-coated Pd nanoparticle are determined to be $3.27 \text{ kcal mol}^{-1}$ and $2.28 \text{ kcal mol}^{-1}$, respectively, which are in good agreement with DFT calculation and experiments. The research demonstrates that the ReaxFF MD simulation is a powerful yet computationally feasible method to study heterogeneous combustion of practical relevance.

Acknowledgments

Support from the Major Project of the National Science Foundation of China (Grant No. 51390493), the China Scholarship Council and the Center for Combustion Energy at Tsinghua University is gratefully acknowledged. The simulations were performed on ARCHER funded under the EPSRC projects “UK Consortium on Mesoscale Engineering Sciences (UKCOMES)” (Grant No. EP/L00030X/1) and “High Performance Computing Support for United Kingdom Consortium on Turbulent Reacting Flow (UKCTRF)” (Grant No. EP/K024876/1). Helpful discussions with Prof. Shuiqing Li of Tsinghua University are also acknowledged.

References

- [1] R.J. Farrauto, M.C. Hobson, T. Kennelly, E.M. Waterman, *Appl. Catal. A: Gen.* 81 (2) (1992) 227–237.
- [2] D. Ciuparu, M. R. Lyubovsky, E. Altman, L.D. Pfefferle, A. Datye, *Cat. Rev.-Sci. Eng.* 44 (4) (2002) 593–649.
- [3] W.R. Schwartz, L.D. Pfefferle, *J. Phys. Chem. C* 116 (15) (2012) 8571–8578.
- [4] T. Shimizu, A.D. Abid, G. Poskrebshev, et al., *Combust. Flame* 157 (3) (2010) 421–435.
- [5] J.H. Lee, D.L. Trimm, *Fuel Process. Technol.* 42 (2) (1995) 339–359.
- [6] T.P. Beebe Jr, D.W. Goodman, B.D. Kay, J.T. Yates Jr., *J. Chem. Phys.* 87 (4) (1987) 2305–2315.
- [7] S.H. Oh, P.J. Mitchell, *Appl. Catal. B-Environ.* 5 (1) (1994) 165–179.
- [8] W. Yarw-Nan, R.G. Herman, K. Klier, *Surf. Sci.* 279 (1) (1992) 33–48.
- [9] R. Prasad, L.A. Kennedy, E. Ruckenstein, *Cat. Rev.-Sci. Eng.* 26 (1) (1984) 1–58.

- [10] L.D. Pfefferle, W.C. Pfefferle, *Cat. Rev.-Sci. Eng.* 29 (2-3) (1987) 219–267.
- [11] M. Lyubovsky, L. Pfefferle, *Appl. Catal. A: Gen.* 173 (1) (1998) 107–119.
- [12] M.J. Lee, N.I. Kim, *Appl. Energy* 87 (11) (2010) 3409–3416.
- [13] D. Ciuparu, M.R. Lyubovsky, E. Altman, L.D. Pfefferle, A. Datye, *A. Catal. Rev. Sci. Eng.* 44 (4) (2002) 593–649.
- [14] T. Zhang, D. Zhu, N. Yao, F. Qi, C.K. Law, *Proc. Combust. Inst.* 33 (2) (2011) 1819–1825.
- [15] Y. Xin, H. Wang, C.K. Law, *Combust. Flame* 161 (4) (2014) 1048–1054.
- [16] R.W. Sidwell, H. Zhu, R.J. Kee, D.T. Wickham, *Combust. Flame* 134 (1) (2003) 55–66.
- [17] R.W. Sidwell, H. Zhu, R.J. Kee, D.T. Wickham, C. Schell, G.S. Jackson, *Proc. Combust. Inst.* 29 (1) (2002) 1013–1020.
- [18] Y. Zong, S. Li, F. Niu, Q. Yao, *Proc. Combust. Inst.* 35 (2) (2015) 2249–2257.
- [19] F. Niu, S. Li, Y. Zong, *J. Phys. Chem. C* 118 (33) (2014) 19165–19171.
- [20] F.H. Ribeiro, M. Chow, R.A. Dallabetta, *J. Catal.* 146 (2) (1994) 537–544.
- [21] M. Lyubovsky, L. Pfefferle, A. Datye, J. Bravo, T. Nelson, *J. Catal.* 187 (2) (1999) 275–284.
- [22] G.B. Hoflund, H. A. Hagelin, J.F. Weaver, G.N. Salaita, *Appl. Surf. Sci.* 205 (1) (2003) 102–112.
- [23] G. Zhu, J. Han, D.Y. Zemlyanov, F.H. Ribeiro, *J. Phys. Chem. B* 109 (6) (2005) 2331–2337.
- [24] T.P. Senftle, R.J. Meyer, M.J. Janik, A.C. van Duin, *J. Chem. Phys.* 139 (4) (2013) 044109.
- [25] A.K. Datye, J. Bravo, T.R. Nelson, P. Atanasova, M. Lyubovsky, L. Pfefferle, *Appl. Catal. A: Gen.* 98 (1) (2000) 179–196.
- [26] T. Griffin, W. Weisenstein, V. Scherer, M. Fowles, *Combust. Flame* 101 (1) (1995) 81–90.
- [27] J.D. Grunwaldt, N. van Vegten, A. Baiker, *Chem. Commun.* (44) (2007) 4635–4637.
- [28] P. Mars, D.W. Van Krevelen, *Chem. Eng. Sci.* 3 (1954) 41–59.
- [29] M. Valden, J. Pere, M. Hirsimäki, S. Suhonen, M. Pessa, *Surf. Sci.* 377(1997) 605–609.
- [30] M. Valden, J. Pere, N. Xiang, M. Pessa, *Chem. Phys. Lett.* 257 (3) (1996) 289–296.
- [31] A. Trincherro, A. Hellman, H. Grönbeck, *Surf. Sci.* 616 (2013) 206–213.
- [32] A. Hellman, A. Resta, N.M. Martin, et al., *J. Phys. Chem. Lett.* 3 (6) (2012) 678–682.
- [33] T. Shimizu, H. Wang, *Proc. Combust. Inst.* 33 (2) (2011) 1859–1866.
- [34] A.C. Van Duin, S. Dasgupta, F. Lorant, W.A. Goddard, *J. Phys. Chem. A* 105 (41) (2001) 9396–9409.
- [35] M. Döntgen, M.-D. Przybylski-Freund, L.C. Kröger, W.A. Kopp, A.E. Ismail, K. Leonhard, *J. Chem. Theory Comput.* 11 (6) (2015) 2517–2524.
- [36] A.V. Akimov, O.V. Prezhdo, *Chem. Rev.* 115 (12) (2015) 5797–5890.
- [37] A.C. Van Duin, A. Strachan, S. Stewman, Q. Zhang, X. Xu, W.A. Goddard, *J. Phys. Chem. A* 107 (19) (2003) 3803–3811.
- [38] T.P. Senftle, M.J. Janik, A.C. van Duin, *J. Phys. Chem. C* 118 (9) (2014) 4967–4981.
- [39] H.M. Aktulga, J.C. Fogarty, S.A. Pandit, A.Y. Grama, *Parallel Comput.* 38 (4) (2012) 245–259.
- [40] W. Humphrey, A. Dalke, K. Schulten, *J. Mol. Graphics* 14 (1) (1996) 33–38.
- [41] J.L. Klepeis, K. Lindorff-Larsen, R.O. Dror, D.E. Shaw, *Curr. Opin. Struct. Biol.* 19 (2) (2009) 120–127.
- [42] K. Honkala, K. Laasonen, *J. Chem. Phys.* 115 (5) (2001) 2297–2302.
- [43] A. Eichler, F. Mittendorfer, J. Hafner, *Phys. Rev. B*, 62, 2000, p. 4744.
- [44] E. Broclawik, J. Haber, A. Endou, et al., *J. Mol. Catal. A: Chem.* 119 (1) (1997) 35–44.
- [45] E. Broclawik, R. Yamauchi, A. Endou, M. Kubo, A. Miyamoto, *Int. J. Quantum Chem* 61 (4) (1997) 673–682.
- [46] M. Van Den Bossche, H. Grönbeck, *J. Am. Chem. Soc.* 137 (37) (2015) 12035–12044.